Published in final edited form as:
J Mol Biol. 2009 October 16; 393(1): 98–112. doi:10.1016/j.jmb.2009.08.023.

Structural basis of HIV-1 activation by NF-kappaB - a higher-order complex of p50:RelA bound to the HIV-1 LTR

James C Stroud[$,@], **Amy Oltman**[#], **Aidong Han**[$], **Darren L. Bates**[#], and **Lin Chen**[$,*]

[$]Molecular and Computational Biology, Department of Biological Sciences, Department of Chemistry, Norris Comprehensive Cancer Center, University of Southern California, Los Angeles, CA 90089-2910

[#]Department of Chemistry and Biochemistry, University of Colorado at Boulder, Boulder, CO 80309-0215

Abstract

The activation and latency of human immunodeficiency virus-1 (HIV-1) is tightly controlled by the transcriptional activity of its long terminal repeat region (LTR). The LTR is regulated by viral proteins as well as host factors, including the nuclear factor kappaB (NF-kappaB) that becomes activated in virus-infected cells. The two tandem NF-kappaB sites of the LTR are among the most highly conserved sequence elements of the HIV-1 genome. Puzzlingly, these sites are arranged in manner that seems to preclude simultaneous binding of both sites by NF-kappaB although previous biochemical work suggests otherwise. Here we have determined the crystal structure of p50:RelA bound to the tandem kappaB element of the HIV-1 LTR as a dimeric dimer, providing direct structural evidence that NF-kappB can occupy both sites simultaneously. The two p50:RelA dimers bind the adjacent kappaB sites and interact through a protein contact that is accommodated by DNA bending. The two dimers clamp DNA from opposite faces of the double helix and form a topological trap of the bound DNA. Consistent with these structural features, our biochemical analyses indicate that p50:RelA binds the HIV-1 LTR tandem kappaB sites with an apparent anti-cooperativity but enhanced kinetic stability. The slow on and off rates we observe may be relevant to viral latency because viral activation requires sustained NF-kappaB activation. Furthermore, our work demonstrates that the specific arrangement of the two kappaB sites on the HIV-1 LTR can modulate the assembly kinetics of the higher-order NF-kappaB complex on the viral promoter. This phenomenon is unlikely restricted to the HIV-1 LTR but probably represents a general mechanism for the function of composite DNA elements in transcription.

Introduction

Human Immunodeficiency Virus-1 (HIV-1) causes acquired immunodeficiency syndrome (AIDS). The progression of AIDS correlates closely with the replication efficiency of HIV-1

*To whom correspondence should be addressed: Molecular and Computational Biology, Department of Chemistry, Norris Comprehensive Cancer Center, University of Southern California, RRI 204C, 1050 Childs Way, Los Angeles, CA 90089-2910. linchen@usc.edu.
[@]Current address: UCLA-DOE Institute for Genomics and Proteomics, Los Angeles, CA 90095-1570

Accession Numbers Coordinates and structure factors have been deposited in the Protein Data Bank with accession number 3GUT.

in infected patients, which in turn is tightly coupled to the transcription of the viral genome. The transcription of HIV-1 is regulated by viral proteins as well as cellular factors of host cells [1; 2; 3; 4; 5; 6; 7; 8; 9; 10]. Although active replication of HIV-1 can be reduced to undetectable levels by antiviral drugs, latently infected memory $CD4^+$ T cells are insensitive to current antiviral chemotherapy and present a major challenge to eradicating HIV-1 virus from infected individuals [11]. The maintenance and reactivation of HIV-1 latency is also tightly controlled by host factors that regulate the silence and re-initiation of viral transcription [12; 13; 14; 15].

The transcription of HIV-1 is initiated from the long terminal repeat (LTR) region of the viral genome. The HIV-1 LTR harbors cis-acting DNA sequences recognized by a variety of host transcription factors [16]. Among these cis-elements, the regulatory region between nucleotides −104 and −180 is the most conserved and extensively characterized [1; 17; 18; 19; 20; 21]. Substantial evidence suggests that this region and the adjacent three Sp-1 sites are important for HIV-1 transcription. The region spanning −104 to −80 contains two consensus NF-kappaB binding sites that are identical to the kappaB site found on the promoter of the immunoglobulin κ (kappa) light-chain gene, also known as the Ig kappaB site. The upstream and downstream kappaB sites on the HIV-1 LTR are referred to as Core II and Core I, respectively [20]. The sequences of the kappaB sites and the 4-nucleotide spacer are highly conserved on most isolates of HIV-1 [16; 21; 22; 23]. Deletion and site-directed mutation of these kappaB sites abolish reporter gene activation driven by the HIV-1 LTR [1; 17; 18; 19; 20; 21]. Despite earlier conflicting results [24; 25], later studies strongly suggest that HIV-1 uses the conserved kappaB sites to enhance its replication in infected host cells [26; 27].

The conservation of kappaB sites on the HIV-1 LTR suggests that NF-kappaB, which is often activated in virally infected cells, may be a key host transcription factor subverted for HIV-1 transcription [1; 10]. Other host factors, such as NFAT1 and NFAT5, have also been implicated in activating HIV-1 transcription through these sites [20; 21; 28; 29; 30], probably allowing HIV-1 to replicate efficiently under different cellular conditions where distinct sets of host factors are activated. Numerous studies have revealed a correlation between the activity of NF-kappaB and LTR-dependent transcription as well as viral growth and replication [9; 12; 13; 14; 15; 31; 32; 33]. Physical association of NF-kappaB with the HIV-1 LTR has also been demonstrated both *in vitro* and *in vivo* [9; 13; 19; 20; 26; 34]. Of the 15 potential NF-kappaB homo- and heterodimers [35; 36; 37], the p50:RelA heterodimer most likely plays the major role in activating the HIV-1 LTR given its abundance in stimulated T cells and the fact that the kappaB sequence (GGGACTTTCC) on the HIV-1 LTR is most optimal for recognition by the p50:RelA heterodimer [38], although p50 homodimer has also been implicated in silencing HIV-1 transcription to promote viral latency through these kappaB sites [12].

The activity of NF-kappaB is inhibited by IkappaB a [39; 40; 41; 42], which is degraded by signals that activate NF-kappaB [43; 44; 45]. The synthesis of IkappaB α in turn is up regulated by NF-kappaB [46]. This negative feedback loop creates intricate oscillation waves of NF-kappaB that can couple specific NF-kappaB activation signals to selective gene expression [47; 48; 49]. Recent studies have shown that activation of the HIV-1 LTR requires sustained NF-kappaB stimulation whereas transient NF-kappaB induction is sufficient to activate some other kappaB-dependent genes [13]. While this unique regulatory property of the HIV-1 LTR could be relevant to the maintenance of HIV latency, its molecular basis is not clear.

A potential clue may reside in the particular arrangement of the tandem kappaB sites on the HIV-1 LTR. Although multiple kappaB sites have been found in a variety of cellular promoters [50], the specific configuration of the tandem kappaB sites conserved on the HIV-1 LTR has not been found in any known host promoters using a relaxed sequence search that identifies a degenerate set of kappaB sites in tandem arrangement between one and six base pairs apart (M. Hartwig and L. Chen, unpublished results). Characterization of kappaB-dependent cellular

genes reveals that multiple kappaB sites on a gene's promoter can act coordinately to exert exquisite control of the expression of target genes [50]. The two kappaB sites on the HIV-1 LTR apparently also function together as mutation of either one of the them dramatically reduces the transcriptional activation of the HIV-1 LTR [1; 2; 18; 19]. *In vitro* binding assays and footprinting suggest that the DNA binding domain and full-length protein of NF-kappaB can bind the tandem kappaB sites simultaneously as a higher-order complex [20; 25].

Most studies probing the function of the tandem kappaB element of the HIV-1 LTR involve mutations of the two kappaB sites or the spacer region. While the majority of the data support the functional importance of this enhancer element in HIV-1 transcription [1; 2; 18; 19; 26; 27], results from a number of mutations in the spacer region are difficult to interpret [14; 19]. A limitation of these mutational studies is that alteration of the tandem kappaB sites and their spacer region may fundamentally change the properties of the HIV-1 LTR such that the behavior of the modified virus may not reflect that of the native virus. Thus, to further study the transcriptional mechanism of the HIV-1 LTR, it is important to characterize the structure and function of host factors bound to these sites. Here we have determined the crystal structure of the DNA binding domain of p50:RelA bound to the HIV-1 LTR tandem kappaB sites as a dimeric heterodimer. This is the first higher-order NF-kappaB complex bound to two adjacent kappaB sites characterized by crystallography. Our structure and accompanying biochemical analyses reveal how DNA binding and protein-protein interaction are coupled together in the assembly of a kinetically stable p50:RelA complex on the HIV-1 LTR. These studies will help understand and further investigate HIV-1 regulation by NF-kappaB in active viral replication and latency, and have general implications for understanding the combinatorial mechanism of eukaryotic gene regulation.

Results

Structure determination and refinement

We have crystallized the heterodimer of the rel homology region (RHR) of human p50 (amino acid residues 39 –350) and RelA (amino acid residues 19 –291, also known as p65) bound to a 26-mer double-stranded DNA containing the tandem kappaB sites from the HIV-1 LTR. The crystals diffracted to 3.6Å resolution. The structure was solved by the molecular replacement method and refined using a strategy taking advantage of previously solved structures of p50:RelA at higher resolutions [51; 52; 53; 54; 55]. After the originalmolecular replacement solution was found using the coordinates from a medium resolution structure [51], we used the protein coordinates from several higher resolution structures of p50:RelA bound to different kappaB elements as a starting point for restrained refinement [52; 53; 54]. After placing the high-resolution structures by least squares fitting, we performed restrained molecular dynamics and minimal rebuilding to obtain the final model. Using the lower resolution coordinates for molecular replacement followed by replacing those coordinates with least-square fitted higher resolution coordinates removed much of the bias from the molecular replacement solution. As a result of this procedure, prior structural knowledge from higher resolution studies is retained in our medium resolution model. The statistics of data collection and refinement are presented in Supplemental Table 1.

Overview of the structure

The asymmetric unit of the crystal contains two independent but nearly identical complexes. The two complexes stack together head to tail through DNA ends and through protein-protein interactions between a p50:RelA dimer on Core I of one complex and another dimer on Core II of the adjacent complex (Figure 1). The DNA forms a pseudo-continuous helix throughout the crystal lattice. Because the p50:RelA dimer forms a nearly complete circle around its DNA substrate, the pseudo-continuous DNA helix is coated by NF-kappaB proteins along almost its

entire length. The crystal packing between adjacent complexes along the DNA axis is reminiscent of that seen in other NF-kappaB/DNA complex crystals [56]. These packing interactions suggest that NF-kappaB dimer may interact with each other to bind DNA cooperatively on adjacent kappaB sites. Our structure, as well as the previously published study of the p50:RelB complex [56], indicates that the two kappaB sites must be arranged in a two-base spacing for this to occur. However, tandem or dyad kappaB sites separated by two base pairs have so far not been found in natural kappaB-dependent promoters, including the HIV-1 LTR, suggesting that the formation of clusters of kappaB sites may not be driven by binding cooperativity but other functional mechanisms.

Structural variation of the p50:RelA dimer

The p50:RelA dimer bound to Core I and Core II resemble each other and the previously determined structures of p50:RelA bound to the same or closely related DNA sequences [51; 52; 53; 54; 55]. The RHR of p50 and RelA consist of two independently folded immunoglobulin domains connected by a flexible linker. The C-terminal domain (RHR-C) mediates dimerization whereas the N-terminal domain (RHR-N) recognizes specific DNA sequences. Using the RHR-C dimerization domain as the reference, which is the most invariant part of NF-kappaB, structural comparison shows that the p50:RelA dimer bound to Core I and Core II differ appreciably in the relative orientation of RHR-N in both p50 and RelA (Figure 2). Similarly, significant difference is also observed in the structural comparison between the p50:RelA dimers bound to the HIV-1 LTR and that bound to an isolated Ig kappaB site [51]. Previous studies have revealed that the conformation of p50:RelA varies upon binding to kappaB sites with different sequences [52; 53; 54]. Such sequence-dependent structural changes have been proposed to confer functional specificity to various kappa sites in vivo [50; 52; 53; 54]. Here we show that the relative orientation of RHR-N and RHR-C of p50:RelA is different even when bound to kappaB sites with the same core sequence but in different promoter contexts and environments. The degree of structural variation observed here is comparable with that observed when comparing p50:RelA bound to kappaB sites of different sequences (data not shown). While this observation complicates the interpretation of the allosteric effects of DNA on the structure and function of bound NF-kappaB [55], it nevertheless suggests that the conformation of the p50:RelA dimer is highly adaptive to surrounding molecular interactions. This adaptation may facilitate the assembly of different NF-kappaB enhancer complexes in different promoter contexts.

DNA structure and indirect readout

The DNA in the crystal structure has well defined electron density, especially at the phosphate backbone (Figure 3a). The structure of the DNA deviates from the ideal B-form in two aspects. First, the DNA contains a significant bend of about 35-degrees in the spacer region between the two kappaB sites (Figure 3b). The center of the bend is located near the 5' end of Core I. Here the major groove of DNA from Gua15 to Gua18 becomes widened, whereas the adjacent minor groove becomes narrowed (Figure 3a). A similar but not identical DNA bend was also observed in the structure of a higher-order NFAT complex bound to the same HIV-1 LTR tandem kappaB sites [30] (Figure 3b), indicating that the spacer region between the two kappaB sites on the HIV-1 LTR has a tendency to bend or an intrinsic bend that can be further remodeled by bound factors.

The second notable DNA deformation occurs in the middle region of the kappaB site of both Core I and Core II. As shown in Figure 3c for Core II, the electron density of base pairs of Ade5-Cyt6-Thy7-Thy8 suggests a cross-strand shift of this region that distorts the standard Watson-Crick base pairing. This structural deformation is also evident from the diagonal offset (over winding) of the DNA backbone. By contrast, the structure of the neighboring DNA bases, including the 5' (Gua2-Gua3-Gua4) and 3' (Thy9-Cyt10-Cyt11) kappaB half sites, are

maintained in a regular B-DNA conformation with standard Watson-Crick base pairing. The DNA in the crystal structure of p50:RelA bound to an isolated Ig kappaB site also shows a severe structural distortion in the middle region of the kappaB site that is characterized by over winding of the backbone and out-of-plane twist of base pairs [51]. The electron density derived from our crystals suggests that base stacking seems to be preserved in both strands, which is energetically more favorable. The staggering of the DNA may establish a new register of base pairing (Figure 4a) or allow bifurcated hydrogen bonds being formed between offset base pairs [57]. Further studies at higher resolutions will be required to analyze the structural details. The middle region of the kappaB site makes few direct contacts to the proteins, so the observed structure changes may serve as a mechanism of indirect readout of DNA by the p50:RelA dimer.

Conservation of DNA binding mechanism

The structures of p50:RelA bound to several different kappa sites have been solved [51; 52; 53; 54; 55]. These structures and related biochemical studies have established a conserved DNA binding mechanism by the p50:RelA dimer. The general features of this mechanism, including dimerization and DNA recognition, are largely conserved in the higher-order complex of p50:RelA bound to the tandem kappaB sites on the HIV-1 LTR. The detailed p50:RelA-DNA interactions in the context of the HIV-1 LTR were analyzed by the program NUCPLOT [58], which made pairing assignments for the distorted middle region of the kappaB site most consistent with a shifted base pairing geometry (Figure 4a). Most of the key DNA binding interactions, such as the recognition of Gua16, Gua17, and Gua18 by the stacked side chains of His364, Arg356 and Arg354 of p50 (Figure 4b), and the recognition of Gua25' and Gua24' by Arg35 and Arg33 of RelA (Figure 4c), are evident from the features of calculated electron density. The well defined electron density at the protein-DNA interface and its consistency with prior knowledge of DNA recognition by the p50:RelA dimer serve as critical validation for the structure and provide us with confidence to interpret the biological implication of other structural features.

The HIV-1 LTR has been analyzed by *in vivo* dimethylsulfate (DMS) footprinting to reveal potential protein contacts under physiological conditions [59; 60]. In these studies, HIV-1 infected T cells were treated with DMS. The resulting footprinting pattern revealed extensive protection of guanine nucleotides in both the Core II and Core I regions, including Gua3, Gua4, Gua6', Gua10', Gua11', Gua16, Gua17, Gua20', Gua24' and Gua25' (Figure 4a). The p50:RelA dimers in our crystal structure contact all of these protected guanines. Interestingly, upon transcriptional activation, the most significant change in the footprinting pattern is an increase in DMS reactivity near Gua15 in the spacer region at the 5' end of Core I. Our structure reveals a significant bend around Gua15, which may explain the enhanced reactivity of this guanine toward DMS. The fact that the DMS hypersensitivity in the spacer region follows activation suggests that the DNA deformation we observe is likely induced by the binding of NF-kappaB or other proteins.

Structural evidence of kinetic stabilization

The p50:RelA dimers bound to Core I and Core II interact with each other through a limited but well defined interface. Here the L1 loop of p50 from the dimer on Core I makes a close contact with the corresponding L1 loop of RelA bound to Core II (Figure 5a). The electron density shows a clear path for the backbone of both loops (Supplemental Figure 1) and some side chain features. A potential assignment of interacting residues at the L1-L1 loop interface is shown in Figure 5b. The interface buries about 246 $Å^2$ of solvent accessible surface and does not show extensive chemical complementarity typically observed in attractive protein-protein interactions. These observations suggest that this loop-loop contact may not contribute to

binding cooperativity but rather affect the assembly of the p50:RelA/HIV-1 LTR complex through other mechanisms.

Modeling using a straight B-DNA of the HIV-1 LTR and the previously determined structure of p50:RelA suggests that two p50:RelA dimers bound to Core I and Core II would clash with each other through their L1 loops (Supplemental Figure 2) [52]. Binding of p50:RelA and the related p50:RelB dimer to the tandem kappaB sites on the HIV-1 LTR show significant anti-cooperativity in that the second dimer binds to the DNA much more weakly than the first dimer [52; 56]. Altering the spacing between the two kappaB sites on artificial synthetic DNA can alleviate the anti-cooperativity [56], probably by removing the clash. On the natural promoter of the HIV-1 LTR observed here, the L1-L1 clash appears to be avoided by DNA bending and by the rigid shift of the RHR-N of p50 on Core I and RelA on Core II (Figure 2). The DNA bends exactly under the L1-L1 loop contact point and in a direction that tilts the adjacent p50 and RelA to accommodate the opposing loops (Figure 5a).

P50:RelA binds isolated Ig kappaB sites with a very high affinity (Kd~10^{-13} to 10^{-10}M) [52; 61], which is equivalent to 17–13 kcal/mole of binding free energy. On the HIV-1 LTR, some of this energy is used to drive conformational changes in DNA and protein, leading to the observed anit-cooperativity in binding assays. While these conformational changes may be important for binding other factors, such as transcriptional co-activators, the relatively high energy cost associated with these structural changes implies a high activation energy barrier of the transition state during the assembly of the p50:RelA/HIV-1 LTR complex, which in turn may lead to enhanced kinetic stability of the assembled complex.

P50:RelA binds DNA like a pair of clamps (Figure 5c). The only exit for DNA is the cleft between the N-terminal domain (RHR-N) of p50 and RelA in the dimer. On the HIV-1 LTR, because the two kappaB sites are separated by about half helical turn, the two clamp-like p50:RelA dimers approach DNA from opposite directions. As a result, the dissociation of the DNA from the cleft of one p50:RelA dimer will be hindered by the nearby dimer (Figure 5c). This trapping effect is further enhanced by the L1-L1 loop contact, which bridges the two dimers (Figure 5d). From the view of protein, the dissociation of one p50:RelA dimer form the DNA will experience hindrance from the nearby dimer. These structural features also suggest that a main effect of binding two p50:RelA dimers to the tandem kappaB sites of the HIV-1 LTR is enhanced kinetic stability of the assembled protein/DNA complex.

Biochemical analyses of the p50:RelA/HIV-1 LTR complex

Similar to that reported in literature [52; 56], we have also observed anti-cooperative binding of p50:RelA to the HIV-1 LTR tandem kappaB sites in electrophoresis mobility shift assay (EMSA). Our structure suggests that a likely cause of the anti-cooperativity is the L1 loop clash described above (Supplemental Figure 2). This clash is consistent with the observation that changing the spacing between the two kappaB sites can alter the binding behavior of the NF-kappaB dimer [56]. To further address this issue on the natural HIV-1 LTR sequence, we deleted residues Glu373, Lys374, Asn375, and Lys376 at the tip of the p50 L1 loop (Figure 5b). This p50Δ373–6 mutant expressed well and formed a heterodimer with the RHR of RelA. The p50Δ373–6:RelA dimer binds the isolated Ig kappaB site with a similar affinity to that of the wild type p50:RelA dimer (data not shown and see below). However, as shown in Figure 6, this mutant dimer showed improved ability to form the higher order complex (lanes 10–19) on the HIV-1 LTR relative to the wild type p50:RelA dimer (lanes 1–9). For p50:RelA, the K_d of binding of the first heterodimer is 1.5 ± 0.22 nM while the K_d of binding of the second heterodimer is 6.4 ± 0.21 nM. For p50Δ373–6:RelA, the K_d of binding of the first heterodimer is 1.51 ± 0.217 nM while the K_d of binding of the second heterodimer is 3.14 ± 0.45 nM. These binding constants indicate that the loop deletion in p50Δ373–6:RelA reduces the anti-cooperative binding observed in wild-type p50:RelA. Comparison between lanes 18–19 and

lanes 8–9 also confirms that the binding energetics of the first dimer to the HIV-1 LTR is similar for the wild type dimer and the p50 deletion mutant, suggesting that the L1 truncation in p50 does not affect appreciably the DNA binding of p50:RelA to isolated kappaB sites.

We measured the dissociation rates of the ternary complex of p50:RelA bound to the wild type HIV-1 LTR tandem kappaB sites and to a mutant probe with three additional base pairs inserted between the two kappaB sites (Figure 7a). To maintain a similar flanking region for each kappaB site, we repeated the spacer sequence GCT to make the insertion mutant. As a control, we also measured the dissociation rate of the p50:relA dimer on an isolated Ig kappaB site. The kinetic dissociation studies involved chasing radiolabeled complexes using excess unlabeled DNA probes. As shown in lanes 2–5 of Figure 7b, the p50:RelA dimer bound to the Ig kappaB site (indicated as dimer in Figure 7b) has a relatively slow dissociation rate compared to most transcription factor/DNA complexes[70]. This slow dissociation rate probably arises from the high affinity binding and the near enclosure of the DNA by the NF-kappaB dimer. On the HIV-1 LTR, the fully assembled p50:RelA dimeric dimer (indicated as tetramer in Figure 7b) is even more kinetically stable (lanes 7–10, Figure 7b), whereas the corresponding complex formed on the insertion mutant is less stable (lanes 12–15, Figure 7b). It should be noted that in lanes 7–10 of Figure 7b, the binary complex on the HIV-1 LTR lasts longer than the complex formed on the isolated Ig kappaB site in the cold chase experiment (lanes 2–5, Figure 7b). This effect is likely due to the slow dissociation of the ternary complex that replenishes the pool of binary complexes consisting of p50:RelA bound to either Core I or Core II..

Quantitative analysis (Figure 7c) of the dissociation data obtained from EMSA indicates that the ternary complex of p50:RelA bound to the wild type HIV-1 LTR ($t_{1/2}$ = 123 ± 5.0 s, Figure 7c, green curve) has a significantly higher kinetic stability than the complex formed on the insertion mutant ($t_{1/2}$ = 55.4 ± 3.7 s, Figure 7c, blue curve). The half life of the p50:RelA dimer bound to the single Ig kappaB site was also calculated ($t_{1/2}$ = 70.2 ± 3.3 s, Figure 7c, red curve). We expect the dissociation half life to be similar for the isolated Ig kappaB site and the insertion mutant if the two p50:RelA dimers bind the two kappaB sites of the insertion mutant independently and in a manner similar to the isolated site. However, under different *in vitro* and *in vivo* conditions, it is possible that the measured kinetic rates of protein/DNA complexes may be affected by other factors such as flanking sequences and experimental conditions [62; 63; 64; 65]. Nevertheless, our data here suggest that the ternary p50:RelA complex assembled on the HIV-1 LTR is more stable than that formed on the isolated kappaB site and on the insertion mutant under our experimental conditions, which is consistent with our structural analyses.

Discussion

A prevalent model of enhanceosome function is cooperative binding of transcription factors to adjacent DNA sites [55; 63; 66; 67]. On the HIV-1 LTR, however, the highly conserved tandem kappaB sites bind p50:RelA and p50:RelB with measurable anti-cooperativity [52; 56]. Our crystal structure reveals that the p50:RelA dimer on Core I and Core II contact each other through their L1 loops. We further show that deletion of the L1 loop of p50 can facilitate the formation of the ternary p50:RelA complex on the HIV-1 LTR, demonstrating that the structural basis of the observed anti cooperativity in EMSA indeed arises from significant structural rearrangements required to avoid a clash of the L1 loops.

A common but peculiar feature of several NF-kappaB structures solved to date is the extended L1 loop that projects away from the immunoglobulin fold. Despite making little contact to the main body of the protein, the L1 loop has a relatively well-defined structure. This loop seems to be poised to interact with DNA in the flanking region and nearby factors [68]. Indeed, as seen

in the beta interferon enhanceosome complex, the L1 loop of p50 makes a small contact to IRF-7 [55]. Here in the p50:RelA/HIV-1 LTR complex, the L1 loop plays a key role to mediate the interaction between two adjacently bound p50:RelA dimers. Our data suggest that the L1-L1 loop contact serves to couple the free energy of DNA binding to conformational changes in the protein/DNA complex, including the bending the DNA and the rigid shift of the RHR-N domains of the interacting p50 and RelA. The conformation of the fully assembled complex may be functionally relevant in recruiting additional factors such as IRF-1or co-activators such as p300/CBP [9].

The amount of free energy involved in driving the conformational change in protein and DNA can be estimated by the Kd difference between the first and second dimer, which is about 1000 fold or 4 kcal/mole [52] (Stroud et al., unpublished data). We expect the intrinsic free energy of DNA binding by each dimer to be similar since we did not observe significant structural differences at the protein/DNA interface between Core I and Core II. The detailed protein/DNA interactions of both dimers are also similar to that seen in the complex of p50:RelA bound to an isolated kappB site [51]. Despite the significant structural rearrangements and the substantial free energy needed to drive these rearrangements, each p50:RelA dimer on the HIV-1 LTR still binds its cognate site in the canonical mode, i.e. we observe no slippage at the protein/DNA interface. The conservation of the DNA binding mechanism also includes structural changes implicated in the indirect readout. These observations suggest that the strong protein/DNA interaction characteristic of NF-kappaB will hold the protein/DNA register in the assembly of the high-order transcription factor complexes [55; 67].

Another potential mechanism of enhanceosome function is through the regulated assembly kinetics of higher-order transcription factor complexes [63; 67; 69; 70]. This mechanism is particularly interesting considering that oscillating NF-kappaB activity has been shown to couple specific stimuli to selective gene expression [47; 48; 49]. Moreover, recent studies have shown that the HIV-1 LTR requires sustained NF-kappaB stimulation for activation whereas transient NF-kappaB activity is sufficient to activate other kappaB-dependent genes [13], but exactly how this selectivity is achieved at the molecular level is not well understood. The assembly kinetics of transcription factor complexes on specific promoter elements may play a key role in this process [71].

A number of observations suggest that the higher-order p50:RelA complex assembled on the HIV-1 LTR have unusual kinetic properties. First, a substantial amount of free energy derived form the DNA binding by the second p50:RelA dimer is apparently used to drive conformational changes in protein and DNA, implicating a high activation energy barrier for the assembly reaction. Second, the two p50:RelA dimers, bridged by the L1-L1 loop contact, form a topological trap around the DNA, similar to that described for RecA [72]. Indeed, we observe that the high-order p50:RelA complex bound to the HIV-1 LTR exhibits more kinetic stability than the complex on isolated kappaB sites and the enhanced kinetic stability depends on the specific juxtaposition of the two kapppaB sites. Although experimental and cellular conditions may influence the measured kinetic rates [72],the effects of varying DNA sequences on the dissociation kinetics of the p50:RelA ternary complex measured under our *in vitro* conditions are consistent with our structural data.

Although transcription factor complexes that bind to composite sites cooperatively might gain kinetic stability through increased affinity [63; 67; 69], the p50:RelA/HIV-1 LTR complex is unique because it displays enhanced kinetic stability despite the anti-cooperative binding of its protein constituents, suggesting that the p50:RelA/HIV-1 LTR complex has an unusual assembly mechanism. Since the second p50:RelA dimer binds the HIV-1 LTR weakly (Kd ~μM) and yet with a slow kinetic off rate (~5×10^{-3} s^{-1}), it follows that the on rate for the second dimer must be even slower (~5×10^{-3} $s^{-1}M^{-1}$). The slow on rate for the second

p50;RelA dimer may explain why the HIV-1 LTR requires sustained NF-kappaB stimulation for activation [13].

Though understanding how the kinetic properties of the p50:RelA/HIV-1 LTR complex are related to the *in vivo* regulation of HIV-1 life cycle await future studies, our data suggest that the organization of the two kappaB sites on the HIV-1 LTR can influence the kinetics of assembly for the higher-order NF-kappaB complex on the LTR. Though our studies are limited to a viral context here, the observation that anticooperativity can influence assembly kinetics probably represents a more general mechanism of combinatorial gene regulation and thus expands the role of composite DNA elements in the genome [66].

A number of host transcription factors, including NF-kappaB, NFAT1, and NFAT5 and have now been shown to bind and activate transcription from the HIV-1 LTR [19; 20; 21; 28]. We have previously shown that NFAT1 can also bind the HIV-1 LTR as both a dimer and a higher-order complex [29; 30]. These systematic structural and biochemical analyses, together with functional data supporting the role of NF-kappaB and NFAT in HIV transcription, suggest that the same promoter enhance element can support the assembly of distinct transcription factor complexes under a variety of cellular conditions.

More than 250 host proteins are shown to be involved in the viral life cycle of HIV-1, many of which represent potential therapeutic targets for AIDS [10]. To explore such an antiviral strategy, it is important to characterize the detailed mechanisms by which host factors are recruited by HIV-1 for viral infection and replication, especially those specific aspects of structure and function of host-viral complexes that may be selectively targeted for intervention. The unique structure and function of the p50:RelA/HIV-1 LTR complex revealed by our studies here could provide a basis for developing therapeutic strategies by inhibiting active viral replication or inducing reactivation of latent virus.

Experimental Procedures

Materials and sample preparation

The p50:RelA dimer was prepared according to previously published procedures with some modifications [51]. Briefly, human p50 (amino acids 39–350) and RelA (amino acids 19–291) were cloned into a pET28a vector and transformed into BL21 (DE3) pLysS for expression by standard procedures. The cells were lysed by sonication in lysis buffer (500mM NaCl, 10mM Hepes, pH 7.7, 10mM β-mercaptoethanol). The cleared lysate was purified over nickel Ni-NTA beads (Qiagen) following the manufacturer's protocol. The eluted protein was further purified on an UNO S6 column (Bio-Rad) with a 10% to 30% NaCl gradient (10mM HEPES, pH 7.7, 5mM β-mercaptoethanol). Both p50 and RelA were purified by the same procedure separately.

To form heterodimers, purified p50 and relA were mixed in a 1:4 (p50:RelA) molar ratio (typically 100 mg of protein total) and denatured in 50mL denaturing buffer (8M urea, 0.5M NaCl, 5mM β-mercaptoethanol) and refolded at 4 °C. Refolding was done with four 6 hr dialysis steps. The first two steps were in high salt refolding buffer (0.5M NaCl, 10mM Tris, pH 7.61, 5mM β-mercaptoethanol) and the second two steps were in low salt refolding buffer (20mM NaCl, 10mM Tris pH 7.61, 5mM β-mercaptoethanol). The refolded complex was again nickel purified as described above, concentrated to 0.5 mL and passed over a HiLoad 16/60 Superdex 200 size exclusion column (Amersham Biosciences #17-1071-01) in storage buffer (150mM NaCl, 5mM DTT, 10 mM Tris pH 7.61) and concentrated to 7–10 mM. The samples were stored at −70 °C in storage buffer containing 20% glycerol. The p50Δ373–6 mutant was made by QuickChange mutagenesis (Stratagene #200518) with the following primers: 5′-CCTGGTGCCTCTAGTAAGTCTTACCCTCAGG-3′ 5′-

CCTGAGGGTAAGACTTACTAGAGGCACCAGG-3′. The p50Δ373–6 was expressed, purified, refolded, and stored with RelA as described for the p50 wild type construct above.

The DNAs used for crystallization and biochemical analyses, including the wild type HIV-1 LTR Core sequence, the insertion mutant, and the isolated Core I, were prepared as described previously [30].

Crystallization, data collection, structure determination and analysis

The p50:RelA/HIV-1 LTR Core DNA complex was prepared by mixing 2:1 equivalents of heterodimer and DNA at a concentration of 16 mg/mL in dilution buffer (10 mM DTT, 100 mM NaCl, 25 mM Tris, pH 7.61). Crystals of the protein/DNA complex were grown at 16 °C by the hanging-drop method using a reservoir buffer of 50mM BTP, pH 6.3, 50mM $CaCl_2$, 7% (w/v) PEG 3K, 1mM spermine, 10mM DTT and 8% (v/v) glycerol. Typically, crystals grew to 200×200×150μm in four to five days. The crystals were indexed in space group $P4_2$, with cell dimensions a=b=167.539 Å, and c=172.56 Å. Crystals were stabilized and cryoprotected by harvesting straight into mother liquor containing 14% (w/v) PEG 3K. All crystals were flash frozen in liquid nitrogen for storage and for data collection under cryogenic conditions (100 K). The data were collected at the Advanced Light Source (ALS, Lawerence Berkeley National Laboratory, Berkeley, CA) beamline 8.2.2 (wavelength 1.0688Å). Data were reduced using DENZO and SCALEPACK [73]. The data is 90.4% complete with an I/σ=26.3 (2.0 for the highest resolution shell). The linear R is 0.082.

The structure of the p50:RelA/HIV-1 LTR Core DNA complex was solved by the molecular replacement method in the $p4_22_12$ space group. We used the structure of p50:RelA/Ig-kappaB complex [51] as a partial model for the rotational search using CNS [74]. Independent rotational search solutions were used for translational search. These searches were combined by model building and subjected to packing analysis by visual inspection. Excellent packing with no clash was seen in two solutions wherein the DNA aligns into a pseudo-continuous helix along two of the 2_1 symmetry axes parallel to *a* and two of the 2_1 symmetry axes parallel to *b* of the unit cell. This initial solution was validated with the phaser program [75]. Because exact rotomers for many side chains can not be confidently placed in the 3.6 Å density, we replaced the lower resolution subunits from 1vkx [51] with higher resolution structures of p50 and RelA from pdb entries 1ikn [76] and 1nfk [77] by least squares fitting followed by minor building and refinement and eventually dropping the symmetry to $p4_2$ so that the refinement could converge.

The electron density for the most part of the structure, including the side chain of bulky residues, is well defined. We used a number of landmarks within the density map to validate our model for the assembly of p50:RelA bound to the HIV-1 LTR. These include the DNA recognition regions (Supplemental Figures 3,4) and the distinctive alpha helices of the p50 and RelA N-terminal domains (Supplemental Figures 5,6). These landmarks provide an unambiguous model for the assembly.

Electrophoresis mobility shift assay

Double stranded DNA fragments were end labeled with ^{32}P with T4-PNK (Promega) and purified by size exclusion chromatography (BioRad Micro Bio-Spin 6). Protein (the p50:RelA and the p50Δ373–6:RelA heterodimers) at varying concentrations was bound to labeled DNA at a concentration of 35 pM. The reactions were allowed to incubate at room temperature for 15 min and then loaded onto a 6% acrylamide gel in 0.5X TBE and ran for 2 hours at 120V. The gel was dried and quantified by phosphor imaging. The K_d was determined from lanes with significant integrated intensities of all three bands by integrating free, singly bound (one heterodimer), and doubly bound (two heterodimers) DNA bands and applying the equation $K_d = [D][P]/[D \cdot P]$ for K_{d1} for the first p50:relAheterodimer, where [D] is the concentration of

the integrated free DNA band, [P] is the free heterodimer in the reaction and [D·P] is the integrated singly bound DNA band. The equation $K_{d2}=[D\cdot P][P]/[D\cdot 2P]$ was used to calculate K_{d2} for the binding of the second p50:relA heterodimer to the D·P complex, where [D·2P] is the integrated doubly bound DNA band.

Measurement of the kinetic stability of complexes

To analyze the dissociation rate, the p50:RelA heterodimer was mixed with ^{32}P labeled DNA (wild type and the insertion mutant) to a final concentration of 65 nM labeled DNA and 156 nM heterodimer in binding buffer (10 mM HEPES, pH 7.4, 100 mM NaCl, 1 mM DTT, 5% glycerol). At time *t=0*, 1000-fold excess of unlabeled DNA was added to compete for heterodimers. At various time points, an aliquot was loaded on a 6% non-denaturing polyacrylamide gel. The bound and unbound DNA probes were separated by electrophoresis and quantified by phosphor imaging. The following equation was used to fit the dissociation curve:

$$\frac{D_t}{D_0}=e^{-k_{off}t}$$

where D_t is the amount of complex normalized by the total input of DNA probe left at time t and D_0 is the amount of complex at time zero. The term k_{off} is the dissociation rate constant. Errors reported are those calculated by the software package KaleidaGraph (Synergy Software) and correspond to error of the curve fit. The k_{off} of p50:RelA from Core I was $9.87 \times 10^{-3} \pm 0.46 \times 10^{-3}$ s^{-1}, from the HIV-1 LTR Core sequence was $5.64 \times 10^{-3} \pm 0.23 \times 10–3$ s^{-1}, and form the HIV-1 LTR Core-insert sequence was $12.5 \times 10^{-3} \pm 0.84 \times 10^{-3}$ s^{-1}.

Supplementary Material

Refer to Web version on PubMed Central for supplementary material.

Acknowledgements

The authors thank Dr. Yongqing Wu, Mark Hartwig, Michael J. Giffin, Wumesh KC for discussion and Steve Edwards for help in data collection. D.L.B and J.C.S. have been supported by an NIH training grant. This research is supported by grants from the NIH (L.C.).

References

1. Nabel G, Baltimore D. An inducible transcription factor activates expression of human immunodeficiency virus in T cells. Nature 1987;326:711–3. [PubMed: 3031512]
2. Siekevitz M, Josephs SF, Dukovich M, Peffer N, Wong-Staal F, Greene WC. Activation of the HIV-1 LTR by T cell mitogens and the trans-activator protein of HTLV-I. Science 1987;238:1575–8. [PubMed: 2825351]
3. Weissman D, Barker TD, Fauci AS. The efficiency of acute infection of CD4+ T cells is markedly enhanced in the setting of antigen-specific immune activation. J Exp Med 1996;183:687–92. [PubMed: 8627183]
4. Levine BL, Mosca JD, Riley JL, Carroll RG, Vahey MT, Jagodzinski LL, Wagner KF, Mayers DL, Burke DS, Weislow OS, Louis DC, June CH. Antiviral effect and ex vivo CD4+ T cell proliferation in HIV-positive patients as a result of CD28 costimulation. Science 1996;272:1939–43. [PubMed: 8658167]
5. Pereira LA, Bentley K, Peeters A, Churchill MJ, Deacon NJ. A compilation of cellular transcription factor interactions with the HIV-1 LTR promoter. Nucleic Acids Res 2000;28:663–8. [PubMed: 10637316]

6. Fenard D, Yonemoto W, de Noronha C, Cavrois M, Williams SA, Greene WC. Nef is physically recruited into the immunological synapse and potentiates T cell activation early after TCR engagement. J Immunol 2005;175:6050–7. [PubMed: 16237100]
7. Choi J, Walker J, Talbert-Slagle K, Wright P, Pober JS, Alexander L. Endothelial cells promote human immunodeficiency virus replication in nondividing memory T cells via Nef-, Vpr-, and T-cell receptor-dependent activation of NFAT. J Virol 2005;79:11194–204. [PubMed: 16103171]
8. Cicala C, Arthos J, Censoplano N, Cruz C, Chung E, Martinelli E, Lempicki RA, Natarajan V, VanRyk D, Daucher M, Fauci AS. HIV-1 gp120 induces NFAT nuclear translocation in resting CD4+ T-cells. Virology 2006;345:105–14. [PubMed: 16260021]
9. Sgarbanti M, Remoli AL, Marsili G, Ridolfi B, Borsetti A, Perrotti E, Orsatti R, Ilari R, Sernicola L, Stellacci E, Ensoli B, Battistini A. IRF-1 is required for full NF-kappaB transcriptional activity at the human immunodeficiency virus type 1 long terminal repeat enhancer. J Virol 2008;82:3632–41. [PubMed: 18216101]
10. Brass AL, Dykxhoorn DM, Benita Y, Yan N, Engelman A, Xavier RJ, Lieberman J, Elledge SJ. Identification of host proteins required for HIV infection through a functional genomic screen. Science 2008;319:921–6. [PubMed: 18187620]
11. Blankson JN, Persaud D, Siliciano RF. The challenge of viral reservoirs in HIV-1 infection. Annu Rev Med 2002;53:557–93. [PubMed: 11818490]
12. Williams SA, Chen LF, Kwon H, Ruiz-Jarabo CM, Verdin E, Greene WC. NF-kappaB p50 promotes HIV latency through HDAC recruitment and repression of transcriptional initiation. Embo J 2006;25:139–49. [PubMed: 16319923]
13. Williams SA, Kwon H, Chen LF, Greene WC. Sustained induction of NF-kappa B is required for efficient expression of latent human immunodeficiency virus type 1. J Virol 2007;81:6043–56. [PubMed: 17376917]
14. West MJ, Lowe AD, Karn J. Activation of human immunodeficiency virus transcription in T cells revisited: NF-kappaB p65 stimulates transcriptional elongation. J Virol 2001;75:8524–37. [PubMed: 11507198]
15. Kim YK, Bourgeois CF, Pearson R, Tyagi M, West MJ, Wong J, Wu SY, Chiang CM, Karn J. Recruitment of TFIIH to the HIV LTR is a rate-limiting step in the emergence of HIV from latency. Embo J 2006;25:3596–604. [PubMed: 16874302]
16. Jeeninga RE, Hoogenkamp M, Armand-Ugon M, de Baar M, Verhoef K, Berkhout B. Functional differences between the long terminal repeat transcriptional promoters of human immunodeficiency virus type 1 subtypes A through G. J Virol 2000;74:3740–51. [PubMed: 10729149]
17. Kawakami K, Scheidereit C, Roeder RG. Identification and purification of a human immunoglobulin-enhancer-binding protein (NF-kappa B) that activates transcription from a human immunodeficiency virus type 1 promoter in vitro. Proc Natl Acad Sci U S A 1988;85:4700–4. [PubMed: 3133660]
18. Perkins ND, Edwards NL, Duckett CS, Agranoff AB, Schmid RM, Nabel GJ. A cooperative interaction between NF-kappa B and Sp1 is required for HIV-1 enhancer activation. Embo J 1993;12:3551–8. [PubMed: 8253080]
19. Kinoshita S, Su L, Amano M, Timmerman LA, Kaneshima H, Nolan GP. The T cell activation factor NF-ATc positively regulates HIV-1 replication and gene expression in T cells. Immunity 1997;6:235–44. [PubMed: 9075924]
20. Cron RQ, Bartz SR, Clausell A, Bort SJ, Klebanoff SJ, Lewis DB. NFAT1 enhances HIV-1 gene expression in primary human CD4 T cells. Clin Immunol 2000;94:179–91. [PubMed: 10692237]
21. Ranjbar S, Tsytsykova AV, Lee SK, Rajsbaum R, Falvo JV, Lieberman J, Shankar P, Goldfeld AE. NFAT5 regulates HIV-1 in primary monocytes via a highly conserved long terminal repeat site. PLoS Pathog 2006;2:e130. [PubMed: 17173480]
22. Verhoef K, Sanders RW, Fontaine V, Kitajima S, Berkhout B. Evolution of the human immunodeficiency virus type 1 long terminal repeat promoter by conversion of an NF-kappaB enhancer element into a GABP binding site. J Virol 1999;73:1331–40. [PubMed: 9882338]
23. Rodriguez MA, Shen C, Ratner D, Paranjape RS, Kulkarni SS, Chatterjee R, Gupta P. Genetic and functional characterization of the LTR of HIV-1 subtypes A and C circulating in India. AIDS Res Hum Retroviruses 2007;23:1428–33. [PubMed: 18184086]

24. Leonard J, Parrott C, Buckler-White AJ, Turner W, Ross EK, Martin MA, Rabson AB. The NF-kappa B binding sites in the human immunodeficiency virus type 1 long terminal repeat are not required for virus infectivity. J Virol 1989;63:4919–24. [PubMed: 2795721]
25. Ross EK, Buckler-White AJ, Rabson AB, Englund G, Martin MA. Contribution of NF-kappa B and Sp1 binding motifs to the replicative capacity of human immunodeficiency virus type 1: distinct patterns of viral growth are determined by T-cell types. J Virol 1991;65:4350–8. [PubMed: 2072454]
26. Alcami J, Lain de Lera T, Folgueira L, Pedraza MA, Jacque JM, Bachelerie F, Noriega AR, Hay RT, Harrich D, Gaynor RB, et al. Absolute dependence on kappa B responsive elements for initiation and Tat-mediated amplification of HIV transcription in blood CD4 T lymphocytes. Embo J 1995;14:1552–60. [PubMed: 7729429]
27. Chen BK, Feinberg MB, Baltimore D. The kappaB sites in the human immunodeficiency virus type 1 long terminal repeat enhance virus replication yet are not absolutely required for viral growth. J Virol 1997;71:5495–504. [PubMed: 9188623]
28. Kinoshita S, Chen BK, Kaneshima H, Nolan GP. Host control of HIV-1 parasitism in T cells by the nuclear factor of activated T cells. Cell 1998;95:595–604. [PubMed: 9845362]
29. Giffin MJ, Stroud JC, Bates DL, von Koenig KD, Hardin J, Chen L. Structure of NFAT1 bound as a dimer to the HIV-1 LTR kappa B element. Nat Struct Biol 2003;10:800–6. [PubMed: 12949493]
30. Bates DL, Barthel KK, Wu Y, Kalhor R, Stroud JC, Giffin MJ, Chen L. Crystal structure of NFAT bound to the HIV-1 LTR tandem kappaB enhancer element. Structure 2008;16:684–94. [PubMed: 18462673]
31. Duh EJ, Maury WJ, Folks TM, Fauci AS, Rabson AB. Tumor necrosis factor alpha activates human immunodeficiency virus type 1 through induction of nuclear factor binding to the NF-kappa B sites in the long terminal repeat. Proc Natl Acad Sci U S A 1989;86:5974–8. [PubMed: 2762307]
32. Griffin GE, Leung K, Folks TM, Kunkel S, Nabel GJ. Activation of HIV gene expression during monocyte differentiation by induction of NF-kappa B. Nature 1989;339:70–3. [PubMed: 2654643]
33. Bachelerie F, Alcami J, Arenzana-Seisdedos F, Virelizier JL. HIV enhancer activity perpetuated by NF-kappa B induction on infection of monocytes. Nature 1991;350:709–12. [PubMed: 2023633]
34. Mukerjee R, Sawaya BE, Khalili K, Amini S. Association of p65 and C/EBPbeta with HIV-1 LTR modulates transcription of the viral promoter. J Cell Biochem 2007;100:1210–6. [PubMed: 17031851]
35. Thanos D, Maniatis T. NF-kappa B: a lesson in family values. Cell 1995;80:529–32. [PubMed: 7867060]
36. Baldwin A Jr. The NF-kappa B and I kappa B proteins: new discoveries and insights. Annu Rev Immunol 1996;14:649–83. [PubMed: 8717528]
37. Hayden MS, Ghosh S. Signaling to NF-kappaB. Genes Dev 2004;18:2195–224. [PubMed: 15371334]
38. Zabel U, Schreck R, Baeuerle PA. DNA binding of purified transcription factor NF-kappa B. Affinity, specificity, Zn2+ dependence, and differential half-site recognition. J Biol Chem 1991;266:252–60. [PubMed: 1985897]
39. Davis N, Ghosh S, Simmons DL, Tempst P, Liou HC, Baltimore D, Bose HR Jr. Rel-associated pp40: an inhibitor of the rel family of transcription factors. Science 1991;253:1268–71. [PubMed: 1891714]
40. Ganchi PA, Sun SC, Greene WC, Ballard DW. I kappa B/MAD-3 masks the nuclear localization signal of NF-kappa B p65 and requires the transactivation domain to inhibit NF-kappa B p65 DNA binding. Mol Biol Cell 1992;3:1339–52. [PubMed: 1493333]
41. Henkel T, Zabel U, van Zee K, Muller JM, Fanning E, Baeuerle PA. Intramolecular masking of the nuclear location signal and dimerization domain in the precursor for the p50 NF-kappa B subunit. Cell 1992;68:1121–33. [PubMed: 1547506]
42. Zabel U, Henkel T, Silva MS, Baeuerle PA. Nuclear uptake control of NF-kappa B by MAD-3, an I kappa B protein present in the nucleus. Embo J 1993;12:201–11. [PubMed: 7679069]
43. DiDonato JA, Hayakawa M, Rothwarf DM, Zandi E, Karin M. A cytokine-responsive IkappaB kinase that activates the transcription factor NF-kappaB. Nature 1997;388:548–54. [PubMed: 9252186]
44. Mercurio F, Zhu H, Murray BW, Shevchenko A, Bennett BL, Li J, Young DB, Barbosa M, Mann M, Manning A, Rao A. IKK-1 and IKK-2: cytokine-activated IkappaB kinases essential for NF-kappaB activation. Science 1997;278:860–6. [PubMed: 9346484]

45. Zandi E, Rothwarf DM, Delhase M, Hayakawa M, Karin M. The IkappaB kinase complex (IKK) contains two kinase subunits, IKKalpha and IKKbeta, necessary for IkappaB phosphorylation and NF-kappaB activation. Cell 1997;91:243–52. [PubMed: 9346241]
46. Sun SC, Ganchi PA, Ballard DW, Greene WC. NF-kappa B controls expression of inhibitor I kappa B alpha: evidence for an inducible autoregulatory pathway. Science 1993;259:1912–5. [PubMed: 8096091]
47. Hoffmann A, Levchenko A, Scott ML, Baltimore D. The IkappaBNF-kappaB signaling module: temporal control and selective gene activation. Science 2002;298:1241–5. [PubMed: 12424381]
48. Covert MW, Leung TH, Gaston JE, Baltimore D. Achieving stability of lipopolysaccharide-induced NF-kappaB activation. Science 2005;309:1854–7. [PubMed: 16166516]
49. Nelson DE, Ihekwaba AE, Elliott M, Johnson JR, Gibney CA, Foreman BE, Nelson G, See V, Horton CA, Spiller DG, Edwards SW, McDowell HP, Unitt JF, Sullivan E, Grimley R, Benson N, Broomhead D, Kell DB, White MR. Oscillations in NF-kappaB signaling control the dynamics of gene expression. Science 2004;306:704–8. [PubMed: 15499023]
50. Leung TH, Hoffmann A, Baltimore D. One nucleotide in a kappaB site can determine cofactor specificity for NF-kappaB dimers. Cell 2004;118:453–64. [PubMed: 15315758]
51. Chen FE, Huang DB, Chen YQ, Ghosh G. Crystal structure of p50/p65 heterodimer of transcription factor NF-kappaB bound to DNA. Nature 1998;391:410–3. [PubMed: 9450761]
52. Chen-Park FE, Huang DB, Noro B, Thanos D, Ghosh G. The kappa B DNA sequence from the HIV long terminal repeat functions as an allosteric regulator of HIV transcription. J Biol Chem 2002;277:24701–8. [PubMed: 11970949]
53. Berkowitz B, Huang DB, Chen-Park FE, Sigler PB, Ghosh G. The x-ray crystal structure of the NF-kappa B p50.p65 heterodimer bound to the interferon beta-kappa B site. J Biol Chem 2002;277:24694–700. [PubMed: 11970948]
54. Escalante CR, Shen L, Thanos D, Aggarwal AK. Structure of NF-kappaB p50/p65 heterodimer bound to the PRDII DNA element from the interferon-beta promoter. Structure (Camb) 2002;10:383–91. [PubMed: 12005436]
55. Panne D, Maniatis T, Harrison SC. An atomic model of the interferon-beta enhanceosome. Cell 2007;129:1111–23. [PubMed: 17574024]
56. Moorthy AK, Huang DB, Wang VY, Vu D, Ghosh G. X-ray structure of a NF-kappaB p50/RelB/DNA complex reveals assembly of multiple dimers on tandem kappaB sites. J Mol Biol 2007;373:723–34. [PubMed: 17869269]
57. Nelson HC, Finch JT, Luisi BF, Klug A. The structure of an oligo(dA).oligo(dT) tract and its biological implications. Nature 1987;330:221–6. [PubMed: 3670410]
58. Luscombe NM, Laskowski RA, Thornton JM. NUCPLOT: a program to generate schematic diagrams of protein-nucleic acid interactions. Nucleic Acids Res 1997;25:4940–5. [PubMed: 9396800]
59. Demarchi F, D'Agaro P, Falaschi A, Giacca M. Probing protein-DNA interactions at the long terminal repeat of human immunodeficiency virus type 1 by in vivo footprinting. J Virol 1992;66:2514–8. [PubMed: 1548776]
60. Demarchi F, D'Agaro P, Falaschi A, Giacca M. In vivo footprinting analysis of constitutive and inducible protein-DNA interactions at the long terminal repeat of human immunodeficiency virus type 1. J Virol 1993;67:7450–60. [PubMed: 8230466]
61. Urban MB, Baeuerle PA. The 65-kD subunit of NF-kappa B is a receptor for I kappa B and a modulator of DNA-binding specificity. Genes Dev 1990;4:1975–84. [PubMed: 2125960]
62. Zabel U, Baeuerle PA. Purified human I kappa B can rapidly dissociate the complex of the NF-kappa B transcription factor with its cognate DNA. Cell 1990;61:255–65. [PubMed: 2184941]
63. Maniatis T, Falvo JV, Kim TH, Kim TK, Lin CH, Parekh BS, Wathelet MG. Structure and function of the interferon-beta enhanceosome. Cold Spring Harb Symp Quant Biol 1998;63:609–20. [PubMed: 10384326]
64. Yie J, Merika M, Munshi N, Chen G, Thanos D. The role of HMG I(Y) in the assembly and function of the IFN-beta enhanceosome. Embo J 1999;18:3074–89. [PubMed: 10357819]
65. Bosisio D, Marazzi I, Agresti A, Shimizu N, Bianchi ME, Natoli G. A hyper-dynamic equilibrium between promoter-bound and nucleoplasmic dimers controls NF-kappaB-dependent gene activity. Embo J 2006;25:798–810. [PubMed: 16467852]

66. Yamamoto, KR.; Pearce, D.; Thomas, J.; Miner, JN. Combinatorial regulation at a mammalian composite response element. In: McKnight, SL.; Yamamoto, KR., editors. Transcriptional Regulation. Vol. Vol. 2. Cold Spring Harbor Laboratory Press; New York: 1992. p. 1169-1192.

67. Chen L, Glover JN, Hogan PG, Rao A, Harrison SC. Structure of the DNA-binding domains from NFAT, Fos and Jun bound specifically to DNA. Nature 1998;392:42–8. [PubMed: 9510247]

68. Muller CW, Rey FA, Sodeoka M, Verdine GL, Harrison SC. Structure of the NF-kappa B p50 homodimer bound to DNA. Nature 1995;373:311–7. [PubMed: 7830764]

69. Jain J, McCaffrey PG, Miner Z, Kerppola TK, Lambert JN, Verdine GL, Curran T, Rao A. The T-cell transcription factor NFATp is a substrate for calcineurin and interacts with Fos and Jun. Nature 1993;365:352–5. [PubMed: 8397339]

70. Yang E, Henriksen MA, Schaefer O, Zakharova N, Darnell JE Jr. Dissociation time from DNA determines transcriptional function in a STAT1 linker mutant. J Biol Chem 2002;277:13455–62. [PubMed: 11834743]

71. Karpova TS, Kim MJ, Spriet C, Nalley K, Stasevich TJ, Kherrouche Z, Heliot L, McNally JG. Concurrent fast and slow cycling of a transcriptional activator at an endogenous promoter. Science 2008;319:466–9. [PubMed: 18218898]

72. Klapstein K, Chou T, Bruinsma R. Physics of RecA-mediated homologous recognition. Biophys J 2004;87:1466–77. [PubMed: 15345529]

73. Minor W, Tomchick D, Otwinowski Z. Strategies for macromolecular synchrotron crystallography. Structure 2000;8:R105–10. [PubMed: 10801499]

74. Brunger AT, Adams PD, Clore GM, DeLano WL, Gros P, Grosse-Kunstleve RW, Jiang JS, Kuszewski J, Nilges M, Pannu NS, Read RJ, Rice LM, Simonson T, Warren GL. Crystallography & NMR system: A new software suite for macromolecular structure determination. Acta Crystallogr D Biol Crystallogr 1998;54:905–21. [PubMed: 9757107]

75. McCoy AJ, Grosse-Kunstleve RW, Adams PD, Winn MD, Storoni LC, Read RJ. Phaser crystallographic software. J. Appl. Cryst 2007;40:658–674. [PubMed: 19461840]

76. Huxford T, Huang DB, Malek S, Ghosh G. The crystal structure of the IkappaBalpha/NF-kappaB complex reveals mechanisms of NF-kappaB inactivation. Cell 1998;95:759–70. [PubMed: 9865694]

77. Ghosh G, van Duyne G, Ghosh S, Sigler PB. Structure of NF-kappa B p50 homodimer bound to a kappa B site. Nature 1995;373:303–10. [PubMed: 7530332]

78. Lavery R, Sklenar H. Defining the structure of irregular nucleic acids: conventions and principles. J Biomol Struct Dyn 1989;6:655–67. [PubMed: 2619933]

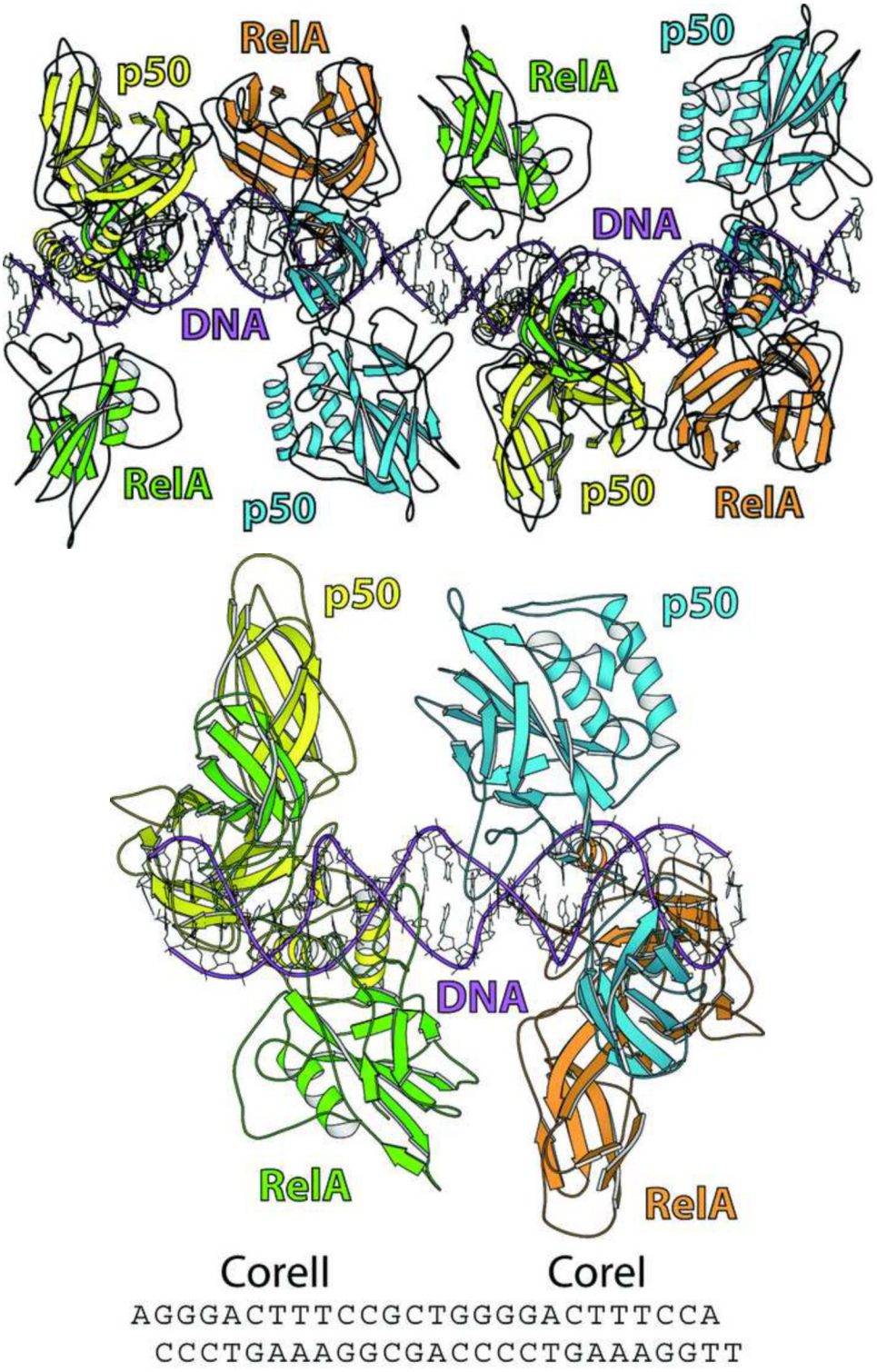

Figure 1.

Structure of the p50:RelA dimer bound to the tandem kappaB sites of the HIV-1 LTR (a) Asymmetric unit. The cyan and orange dimers are bound to the two copies of Core I and the yellow and green dimers are bound to Core II. Protein is shown in ribbons and DNA is shown as sticks with magenta ribbon tracing the phosphate backbone. Yellow: p50 on Core II, green:

RelA on Core II, cyan: p50 on Core I, orange: RelA on Core I. (b) Biological unit. Protein and DNA representations are as in Figure 1a. The sequence of the DNA is shown below the structure.

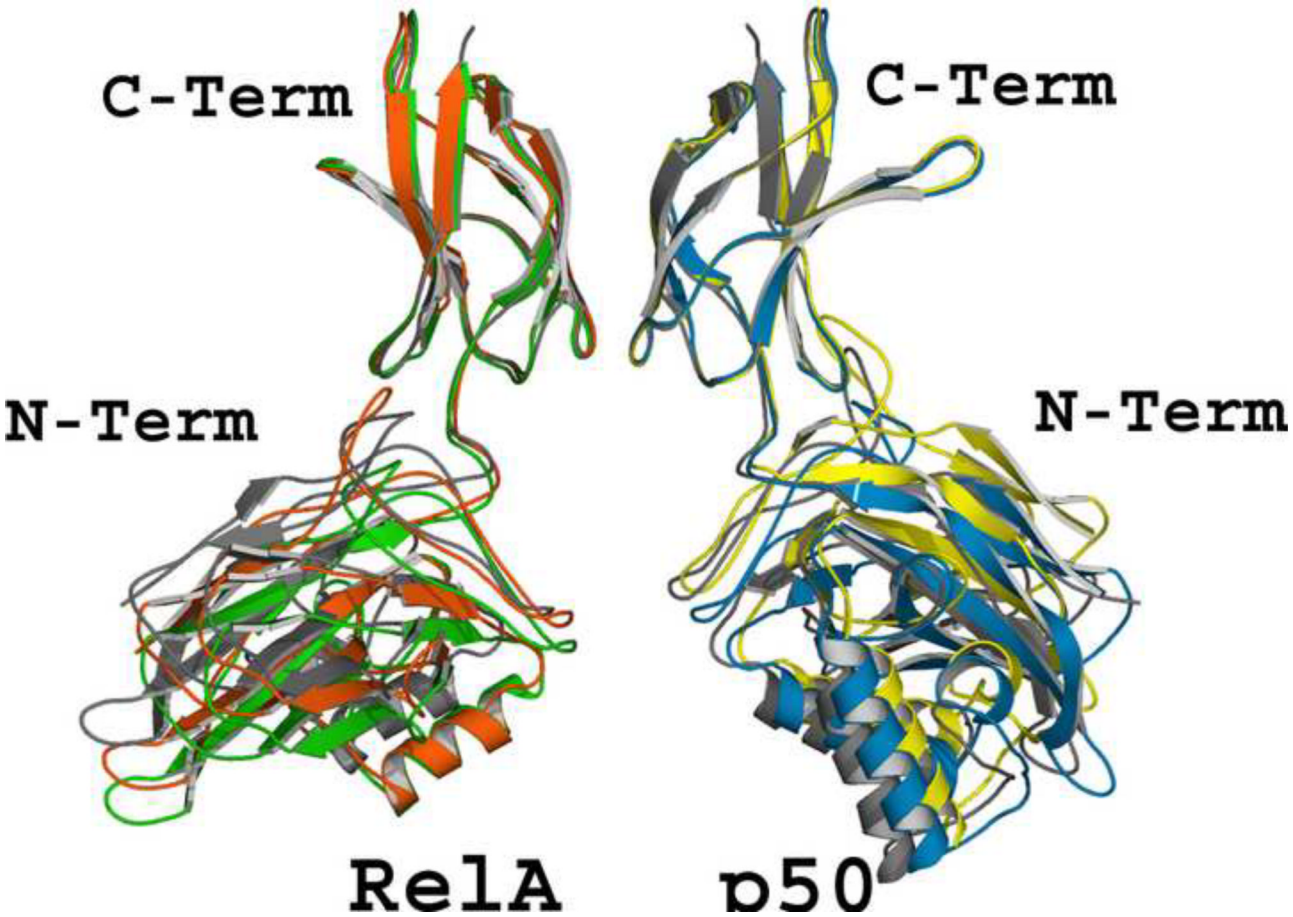

Figure 2.
Comparison of the p50:RelA dimer bound to Core I, Core II, and an Ig kappaB site. The dimers are aligned by least-squares fitting of their C-terminal domains. Yellow: p50 on Core II, green: RelA on Core II, cyan: p50 on Core I, orange: RelA on Core I. The p50:RelA dimer on the isolated Ig kappaB site is colored in gray. The p50 and RelA subunits are labeled together with their N- and C-termini. The p50 subunit is on the right and the RelA subunit is on the right and p50 is on the left. The DNA is omitted in this view.

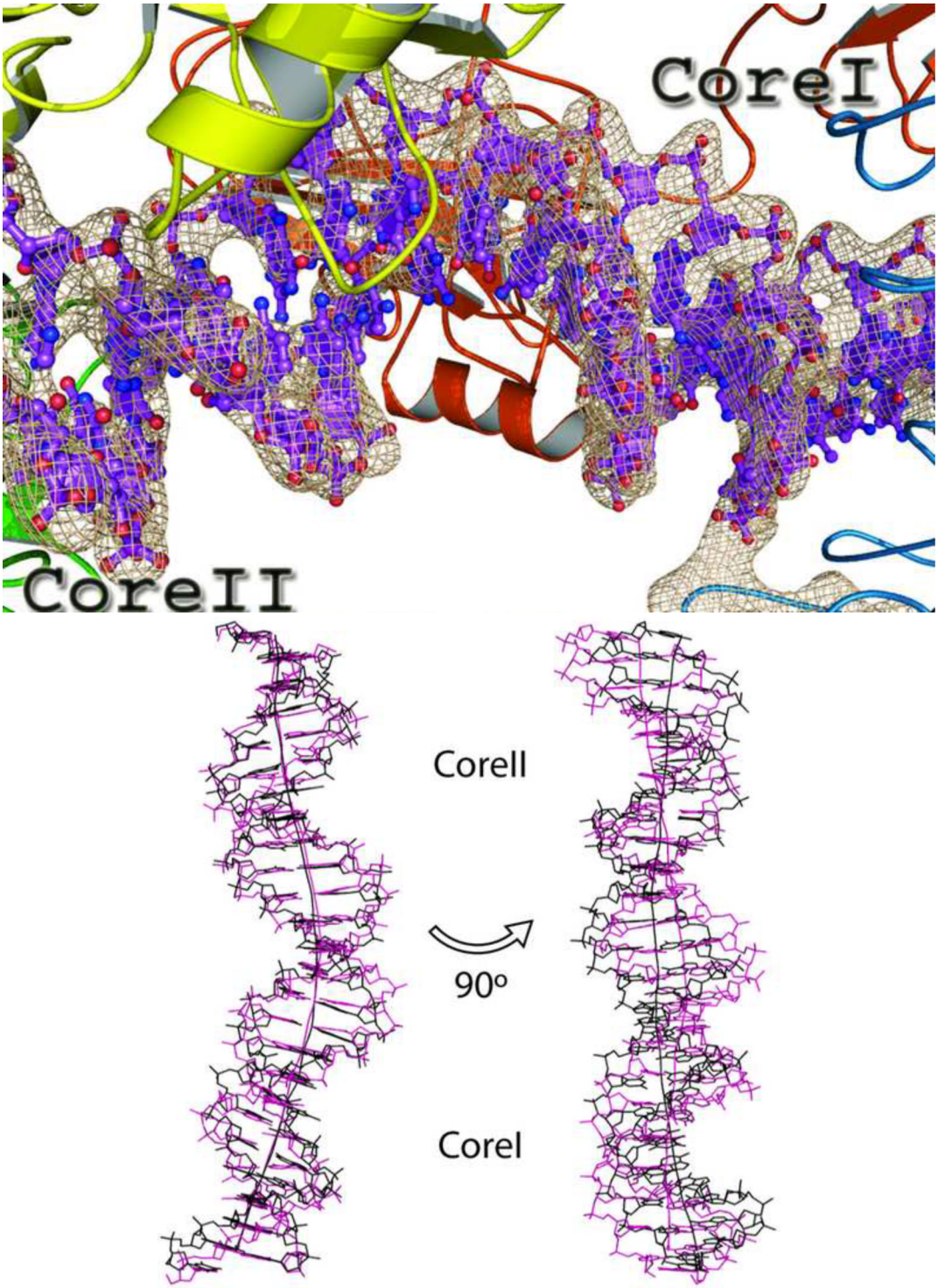

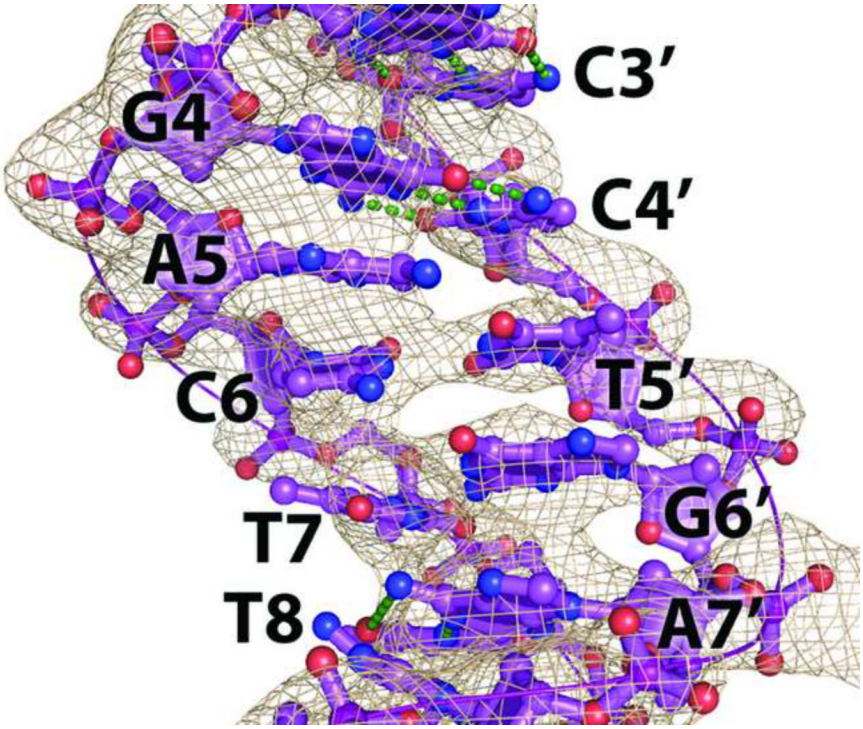

Figure 3.

DNA structure and indirect readout by the p50:RelA dimer on the HIV-1 LTR (a) Electron density of DNA in the region of the bend. The sigma-a weighted DNA density is well defined. Knobs in the density, observable around the tetrahedrally arranged red oxygen atoms which correspond to backbone phosphate groups, combined with the absence of a knob at the 5' ends of the DNA (not shown) establish two possible orientations of the DNA in the asymmetric unit. General agreement with the base density combined with prior knowledge of protein-DNA recognition [51] disambiguates these two possibilities. The DNA is colored in magenta. Yellow: p50 on Core II, green: RelA on Core II, cyan: p50 on Core I, orange: RelA on Core I. (b) Comparison of the LTR tandem kappaB DNA from the NFAT1 (black) and NF-kappaB (magenta) bound structures [30]. The DNA was aligned by least squares fitting of the phosphorous atoms of both DNAs. The superposed DNA on the left are oriented to show the direction of the largest bend. In this direction, the bend (shown as an axis made by a five point spline by CURVES) [78] of the two DNAs follow each other nearly perfectly. The DNA on the right are rotated 90 degree around the vertical axis of the illustration. Core I is oriented towards the bottom of the figure and Core II is towards the top. (c) Sigma-a weighted 3fo2fc density at 3 e/Å^3 in the region between p50 and RelA on Core II. Proteins are excluded from the figure for clarity. Hydrogen bonding inferred from Watson-Crick pairing is shown as green dashes for visual reference although the resolution does not allow assignment of hydrogen bonding.

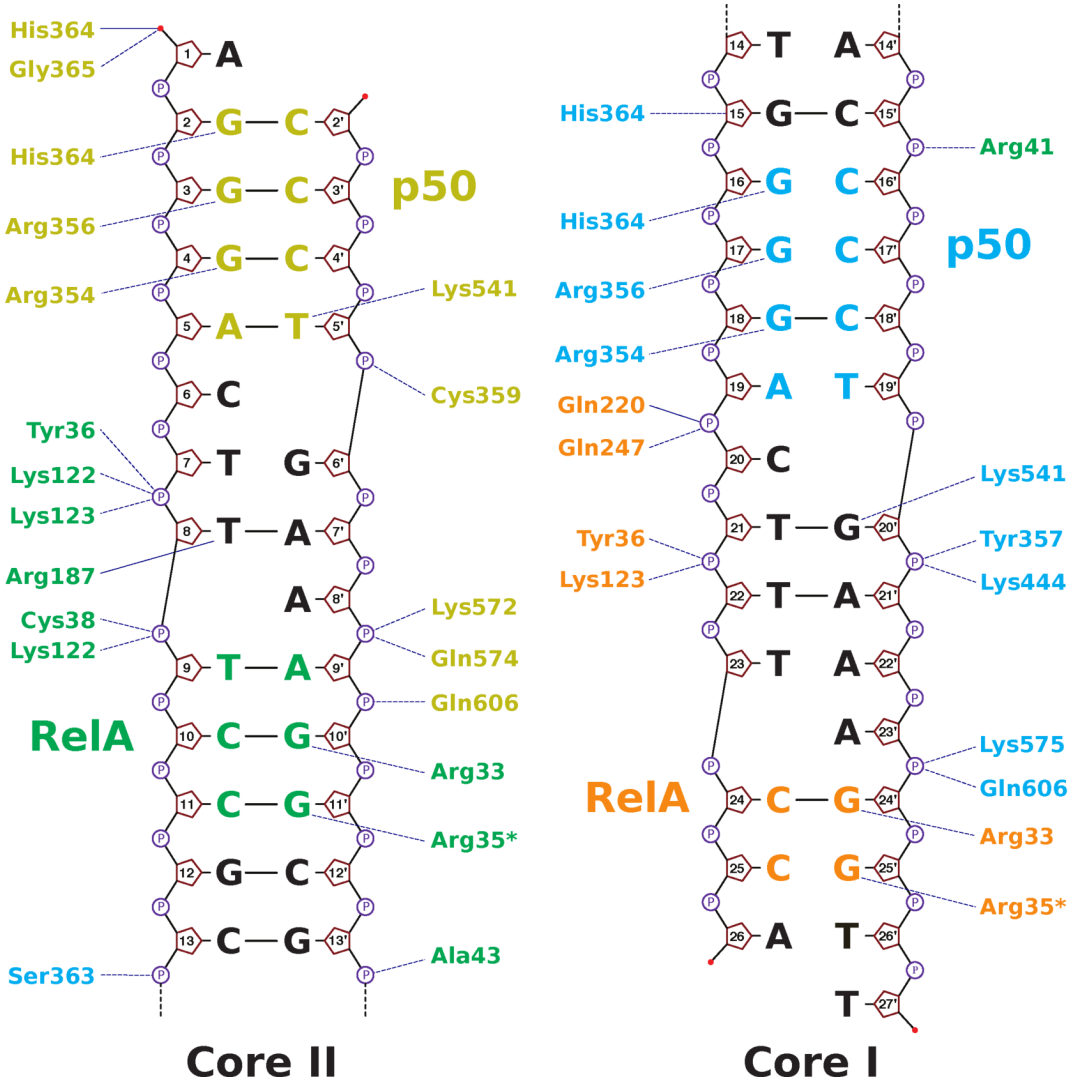

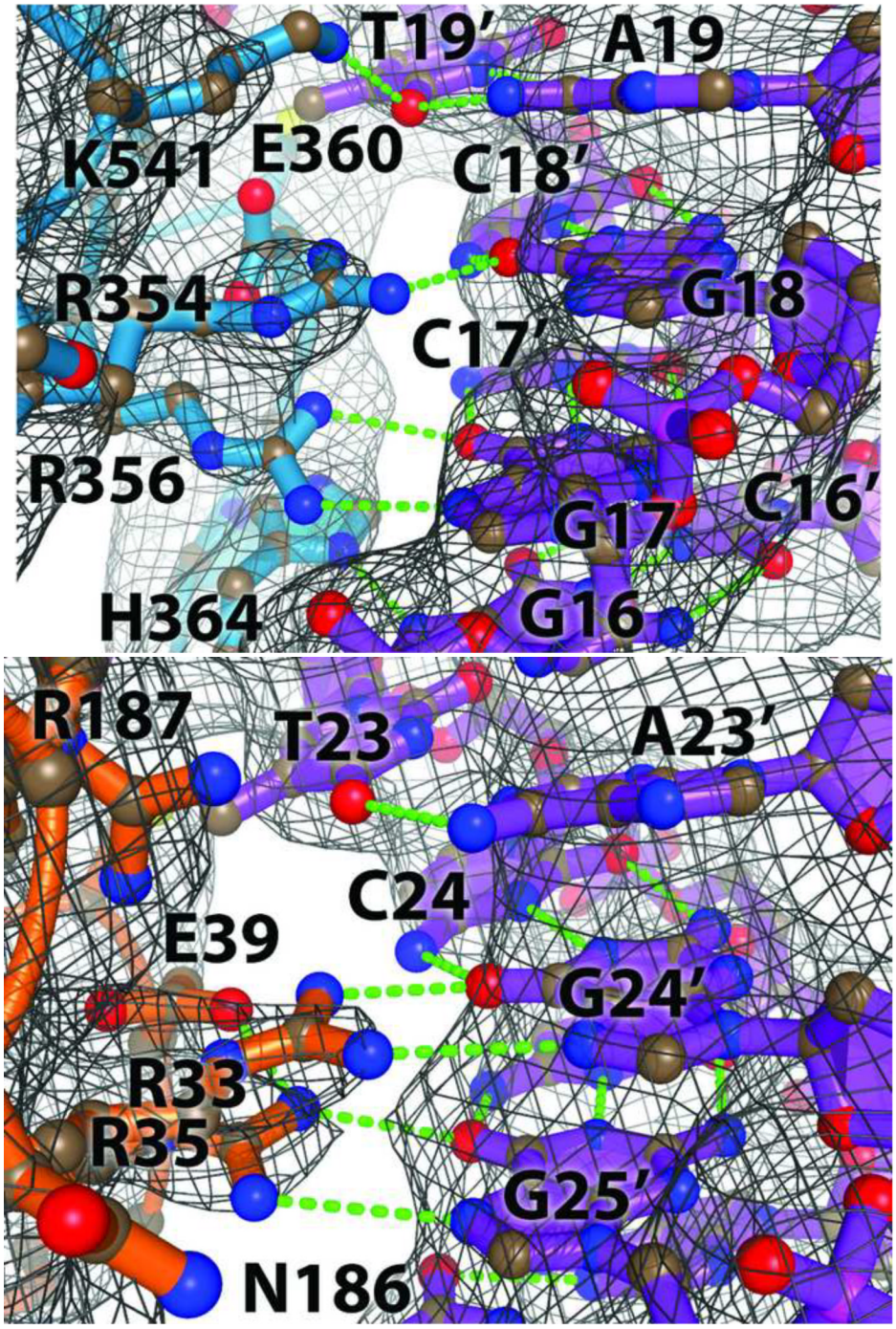

Figure 4.

Conservation of the DNA binding mechanism of p50:RelA dimer on the HIV-1 LTR (a) Schematic of protein-DNA interactions. All assignments are by NUCPLOT [58]. Protein residues are colored as following: yellow, p50 of Core II; green, RelA of Core II; cyan, p50 of Core I; orange: RelA of Core I. The binding sites on the DNA are colored according to their cognate protein. Lines between bases represent proximity of the bases close enough to allow Watson-Crick hydrogen bonding, but do not necessarily represent actual Watson-Crick bonding as the resolution does not allow specific assignment of hydrogen bonds. (b) Sigma-a weighted 3fo2fc

electron density of p50-Core I protein-DNA recognition at 0.5 e/Å^3. The presence of clear electron density for several key head-groups, such as Arg354, Arg356, and His364, helps to establish that the protein in this area is p50 (cyan). Hydrogen bonding is assigned using prior knowledge of p50-DNA recognition and is shown as green dashes [51]. Density is shown as grey mesh. (c) Sigma-a weighted 3fo2fc electron density of RelA-Core I protein-DNA recognition at 0.5 e/Å^3. The presence of clear electron density for several key head-groups, such as Arg33 and Arg35 helps to establish that the protein in this area is RelA (orange). Hydrogen bonding is assigned using prior knowledge of RelA-DNA recognition [51] and is shown as green dashes. Density is shown as grey mesh.

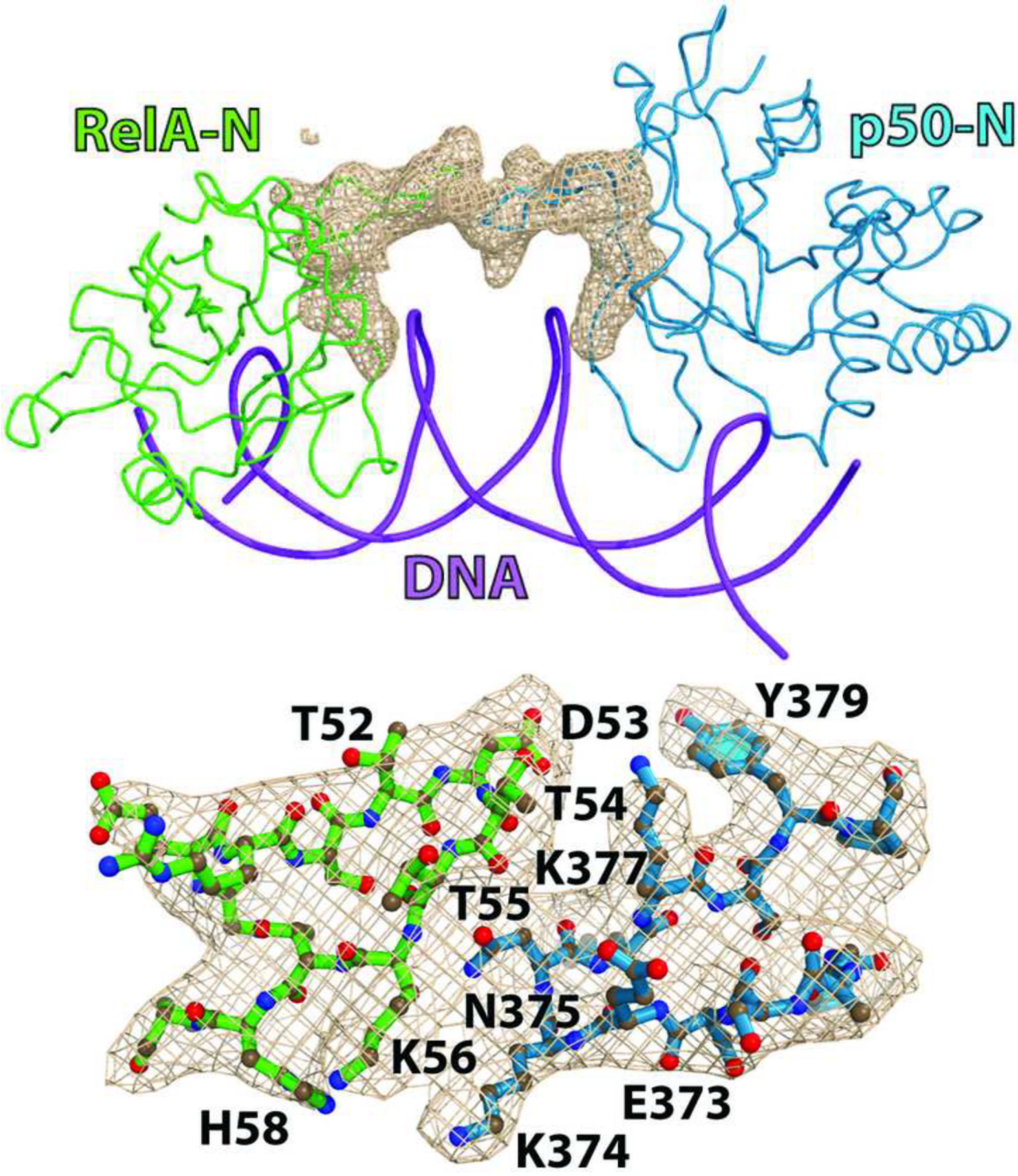

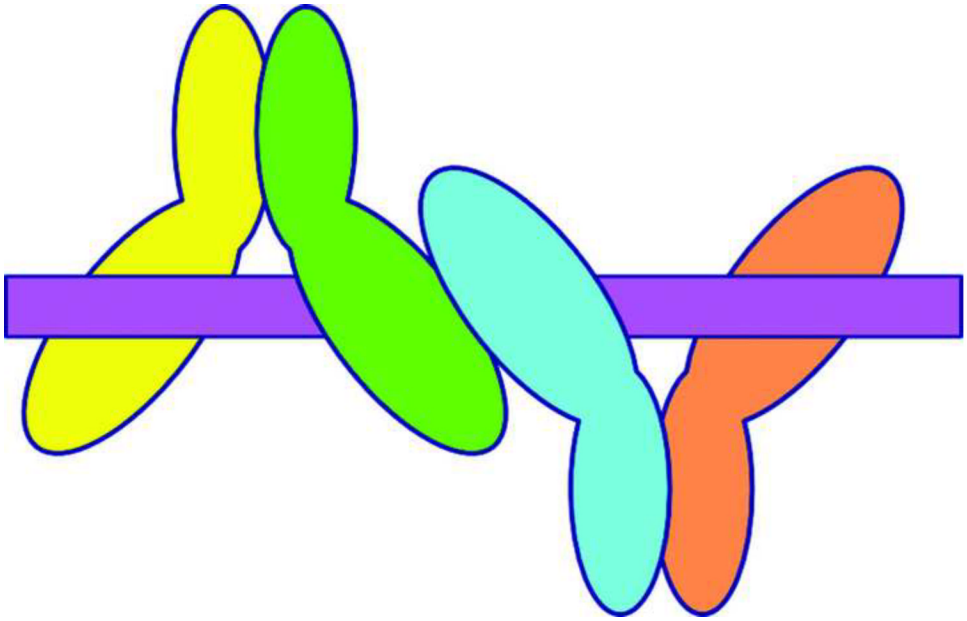

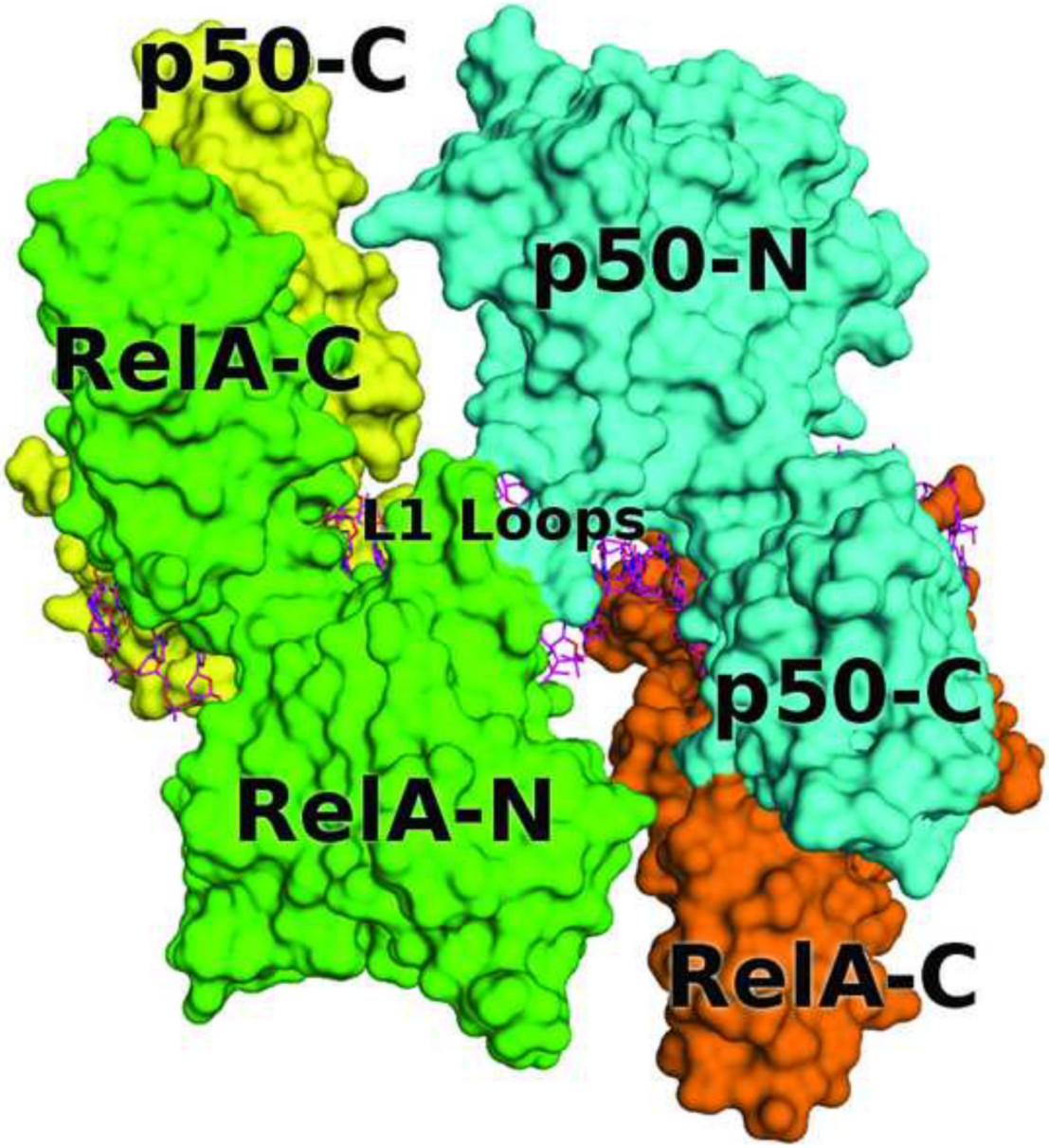

Figure 5.

The two p50:RelA dimers form a topological trap of the DNA on the HIV-1 LTR (a) Simulated annealing omit fofc map of electron density at 1.5 e/Å^3 in the region of the L1 loops. The N-terminal domain of p50 on Core I (cyan) and RelA on Core II (green) are shown as backbone traces. DNA is shown as a cartoon (magenta). This view shows clearly that the DNA bends underneath the L1 loops and away from the protein interface. (b) A zoom-in top view of the electron density map at the L1-L1 interface. A potential assignment of interacting residues was made based on the side chain features of bulky residues. Coloring is as in Figure 1a. (c) A schematic illustration of the topological trap formed by the two interacting p50:RelA dimers bound to the HIV-1 LTR tandem kappaB sites. (d) A surface model of the p50:RelA/HIV-1 LTR complex showing that the DNA is trapped by the higher-order protein complex. The orientation and coloring is the same as Figure 1b.

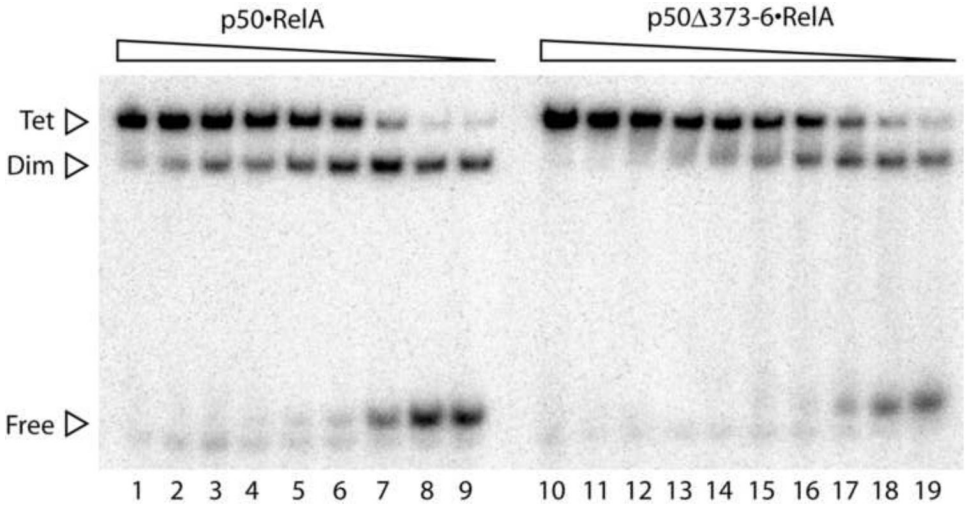

Figure 6.

Truncation of the L1 loop of p50 reduces the anti-cooperativity of p50:RelA to the HIV-1 LTR Electrophoresis mobility shift assay of p50:RelA or p50Δ373–6:RelA bound to the HIV-1 LTR tandem kappaB sites. Protein is titrated in from right to left in 1.5 fold increases of protein concentration. Lane 9 contains 205 pM of p50:RelA. Lane 19 contains 479 pM of p50Δ373–6:RelA. The DNA concentration was kept at 35 pM for all binding reactions. Tet: dimeric heterodimer bound to DNA; Dim: heterodimer bound to DNA; Free: unbound DNA.

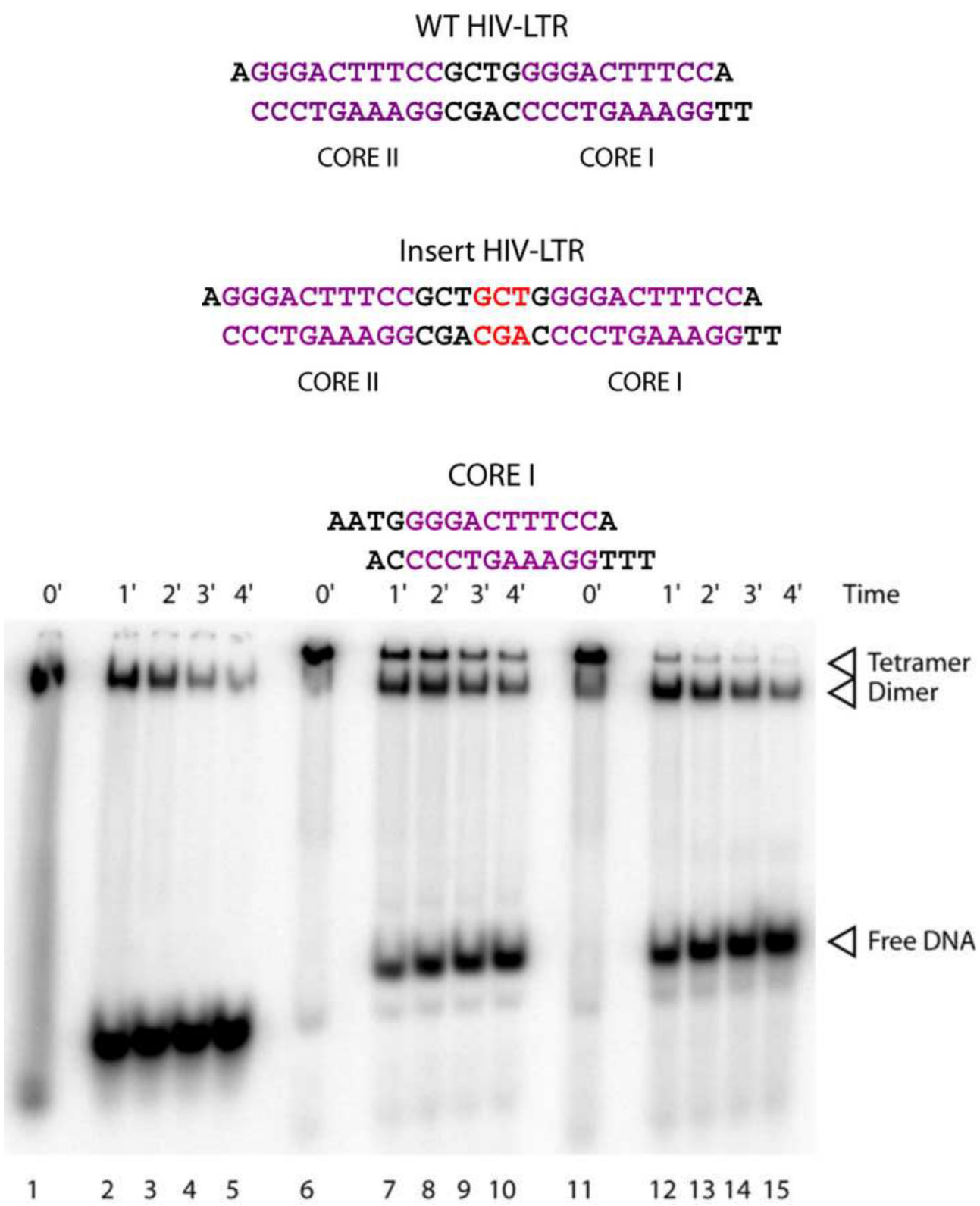

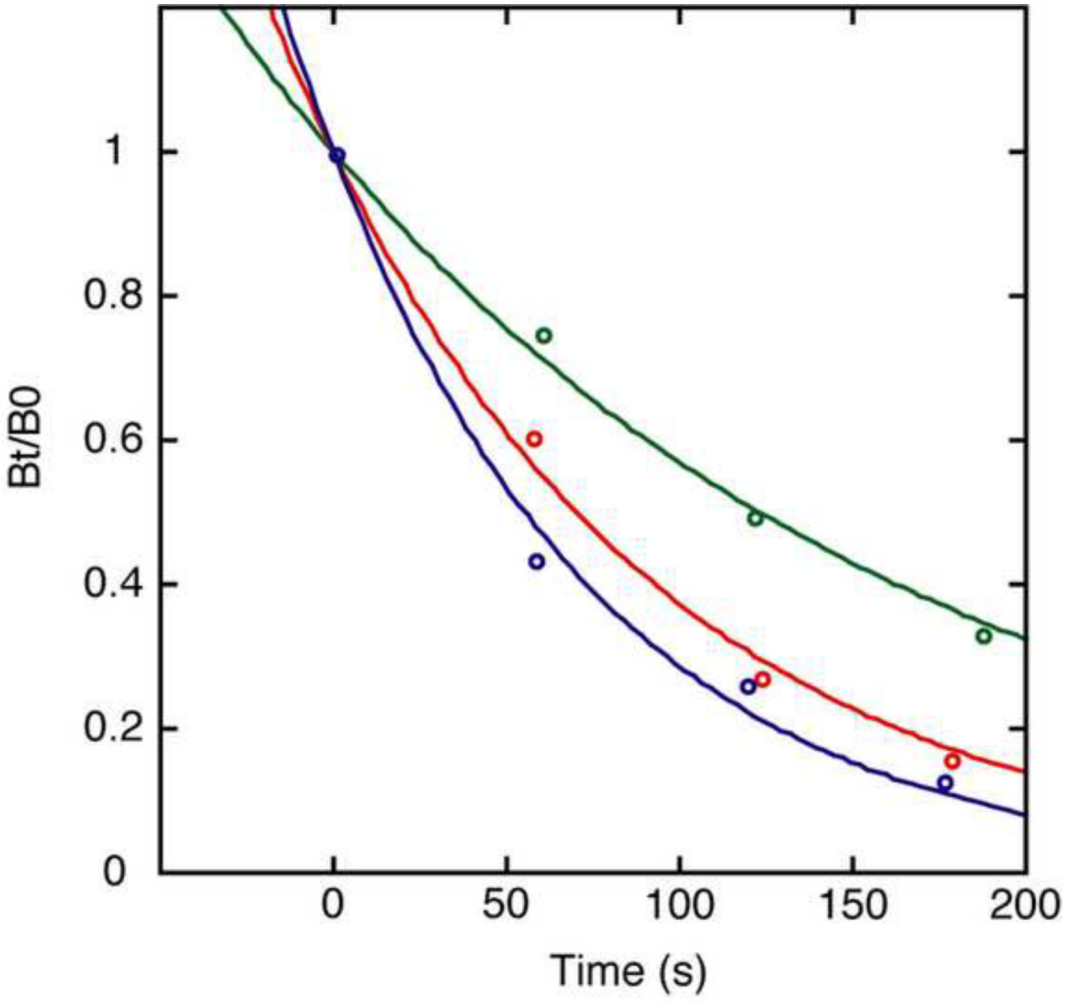

Figure 7.

Kinetic analysis of the p50:RelA/HIV-1 LTR complex (a) DNA sequences used in this study. The p50:RelA sites are shown in violet and the inserted residues are in red. (b) Cold chase of radiolabeled complexes. Time with competitor (see Methods) is indicated above the lanes. Lanes 1–5: p50:RelA bound to isolated Core I only; lanes 6–10: p50:RelA bound to the wild type HIV-1 LTR tandem kappaB sites; lanes 11–15: p50:RelA bound to the HIV-1 LTR insert mutant. The dimeric heterodimer of p50:RelA is indicated as “Tetramer”. (c) Dissociation kinetics data. The ordinate, “Bt/B0”, is the fraction bound at time *t* divided by the fraction bound at time 0 s. The abcissa is the time with competitor DNA. The red curve is the dissociation of the p50:RelA heterodimer from the isolated Core I DNA. The blue curve is the dissociation of the dimeric heterodimer band from the HIV-1 LTR insert mutant. The green curve is the dissociation of the dimeric heterodimer band from the wild type HIV-1 LTR sequence.